

Light scalar spectrum in a graviton soft wall model

Matteo Rinaldi¹

¹Università degli studi di Perugia, Dipartimento di Fisica e Geologia.
INFN Sezione di Perugia. Via A. Pascoli, 06123, Perugia, Italia.
Vicente Vento²

² Departamento de Física Teórica-IFIC, Universidad de Valencia- CSIC,
46100 Burjassot (Valencia), Spain.

Abstract

In this study we present a unified phenomenological analysis of the scalar glueball and scalar meson spectra within an AdS/QCD framework in the bottom up approach. For this purpose we generalize the recently developed graviton soft-wall (GSW) model, which has shown an excellent agreement with lattice QCD glueball spectrum, to a description of glueballs and mesons with a unique energy scale. In this scheme, dilatonic effects, are incorporated in the metric as a deformation of the AdS space. Besides their spectra, we also discuss the mixing of scalar glueball and scalar meson states in the GSW model. To this aim, the light-front holographic approach, which connects the mode functions of AdS/QCD to the light-front wave functions, is applied. This relation provides the probabilistic interpretation required to properly investigate the mixing conditions.

1 Introduction

In the last few years, hadronic models, inspired by the the holographic conjecture [1, 2], have been vastly used and developed in order to investigate non-perturbative features of glueballs and mesons, thus trying to grasp fundamental features of QCD [3, 4]. Recently we have used the so called AdS/QCD models to study the glueball spectrum [5, 6]. The holographic principle relies in a correspondence between a five dimensional classical theory with an AdS metric and a supersymmetric conformal quantum field theory with $N_C \rightarrow \infty$. This theory, different from QCD, is taken as a starting point to construct a 5 dimensional holographic dual of it. This is the so called bottom-up approach [7, 8, 9, 10]. To do so models are constructed by modifyng the five dimensional classical AdS theory with the aim of resembling QCD as much as possible. The main differences characterising these models are related to the strategy used to break conformal invariance. Moreover, their predictions for observable are leading order in the number of colours expansion. For example, the meson masses are $\mathcal{O}(N_C^0)$, thus these models reproduce the essential features of the meson spectrum [11, 12, 13]. Let us mention that for mesons and baryons, the AdS/QCD approaches have been successfully used to describe form factors and various types of parton distribution functions [13, 14, 15, 16]. Within this formalism, also the glueball masses, being $\mathcal{O}(N_C^0)$, have been studied [6, 17, 18].

In this investigation, we start from the so called soft-wall (SW) models, were a dilaton field is introduced to softly break conformal invariance. The SW models have been proven very successful in reproducing both the meson and the glueball properties. Recently we have introduced a model, the graviton soft-wall model (GSW) [6, 19], which has been able to describe the lattice QCD glueball spectrum [20, 21, 22], whose slope was not reproduced by the traditional SW models. In here, we generalize the GSW model to study also the scalar mesons, known as the f_0 mesons [23, 24], particles with spin parity $J^{PC} = 0^{++}$. In the next section we discuss the bottom-up approach of the AdS/QCD correspondence [7, 8, 9], and describe the generalization of the GSW model [6] to describe both the glueballs and the mesons in the same model and with a unique energy scale. In section III we discuss glueball-meson mixing and finally in the conclusions we extract some consequences of our analysis.

2 Scalar glueball and scalar meson spectrum in the graviton soft-wall model

The GSW model describes quite well the scalar glueball spectrum [6] of quantum gluodynamics (QGP). However, the conventional SW models based on the AdS_5 metric do not lead to a good simultaneous description of the

glueball and meson spectra. We show next that if we generalize the metric incorporating an exponential factor $e^{\alpha\varphi(z)}$ the GSW model achieves that goal. These kind of modifications have been adopted in several improvements of the SW model, see Refs. [17, 18, 25, 26]. Thus the metric to be used is,

$$ds^2 = \frac{R^2}{z^2} e^{\alpha\varphi(z)} (dz^2 + \eta_{\mu\nu} dx^\mu dx^\nu) = \frac{R^2}{z^2} e^{\alpha\varphi(z)} g_{MN} dx^M dx^N = \bar{g}_{MN} dx^M dx^N. \quad (1)$$

The function $\varphi(z)$ will be specified later and the need for α will become apparent in the next subsections. In what follows quantities evaluated in the GSW model are displayed with bar. The relation between the standard AdS_5 metric and \bar{g}_{MN} is

$$\bar{g}^{MN} = e^{-\alpha\varphi(z)} g^{MN}, \quad (2)$$

$$\sqrt{-\bar{g}} = e^{\frac{5}{2}\alpha\varphi(z)} \sqrt{-g}. \quad (3)$$

Having introduced this metric we define the GSW action in the scalar sector as

$$\bar{I} = \int d^5x \sqrt{-\bar{g}} e^{\beta\varphi(z)} [\bar{g}^{MN} \partial_M S(x, z) \partial_N S(x, z) + M_{5m}^2 S^2(x, z)], \quad (4)$$

where $R^2 M_{5m}^2 = -3$ is the AdS_5 mass of the scalar meson, $S(x, z)$ the scalar meson field and $e^{\beta\varphi(z)}$ is a dilaton used to describe the soft-wall behavior. In terms of the standard AdS_5 metric, this action becomes

$$\bar{I} = \int d^5x \sqrt{-g} e^{\varphi(z)(\frac{3}{2}\alpha + \beta)} [g^{MN} \partial_M S(x, z) \partial_N S(x, z) + e^{\alpha\varphi(z)} M_{5m}^2 S^2(x, z)]. \quad (5)$$

From the Einstein's equation corresponding to the metric Eq. (1), the scalar glueball equation of motion (EoM) and relative spectra. From the action Eq. (5), the scalar meson equation of motion and spectra have been derived via the variation of the scalar field. The metric of our model will be defined by choosing

$$\varphi(z) = kz^2. \quad (6)$$

where k is the scale factor determined by the fitting the meson spectrum within the SW model [12, 18]. The parameter β is fixed by imposing that $\frac{3}{2}\alpha + \beta = -1$. Such a relation ensures that the kinetic term for the scalar meson is the same of that described in the standard SW model. This ansatz was crucial to reproduce the Regge behavior in the meson sector [6, 10, 11]. Thus the parameters α and β can be interpreted as the relative amount of dilatonic effects shared by the metric and the dilaton field interacting with the scalar field.

In the present analysis, we start by fitting the lattice glueball spectrum with the mass equation obtained from the Einstein equation for the graviton [6]. The fit will fix the product αk . We next proceed to fit the PDG scalar meson spectrum with the mass equation derived from the EoM coming from the action for the scalar fields. This fit will lead to separate values for α and k .

2.1 Glueballs

The Einstein equations, for the metric Eq. (1), lead to the glueball mode equation in the 5th-variable z once the x dependence has been factorized as $\Phi(z) e^{ix_\mu q^\mu}$, where $q^2 = -M^2$ and M represents the mass of the glueball modes

$$\frac{d^2\Phi(z)}{dz^2} - \left(\alpha kz + \frac{3}{z} \right) \frac{d\Phi(z)}{dz} + \left(\frac{8}{z^2} - 6\alpha k - 4\alpha^2 k^2 z^2 + M^2 \right) \Phi(z) - \frac{8}{z^2} e^{\alpha kz^2} \Phi(z) = 0, \quad (7)$$

By performing the change of function

$$\Phi(z) = e^{\alpha kz^2/4} \left(\frac{z}{\alpha k} \right)^{\frac{3}{2}} \phi(z) \quad (8)$$

we get a Schrödinger type equation

$$-\frac{d^2\phi(z)}{dz^2} + \left(\frac{8}{z^2} e^{\alpha kz^2} - \frac{15}{4} \alpha^2 k^2 z^2 + 7\alpha k - \frac{17}{4z^2} \right) \phi(z) = M^2 \phi(z). \quad (9)$$

In this equation it is apparent that M^2 represent the mode mass squared which will arise from the eigenvalues of an *Hamiltonian* operator scheme.

It is convenient to move to adimensional variables $t = \sqrt{\alpha k/2} z$ and we define the mode by $\Lambda^2 = (2/\alpha k) M^2$. The the equation becomes

$$-\frac{d^2\phi(t)}{dt^2} + \left(\frac{8}{t^2}e^{2t^2} - 15t^2 + 14 - \frac{17}{4t^2} \right) \phi(t) = \Lambda^2\phi(t). \quad (10)$$

This is a typical Schrödinger equation with no free parameters except for an energy scale in the mass determined by αk . The potential term is uniquely determined by the metric and only the scale factor is unknown and will be determined from lattice QCD. This equation has no exact solutions and numerical solutions can be found [6]. One can be tempted to make the approximation

$$\frac{e^{2t^2}}{t^2} = \frac{1}{t^2} + 2 + 2t^2, \quad (11)$$

which leads to

$$-\frac{d^2\phi(t)}{dt^2} + \left(t^2 + 30 + \frac{15}{4t^2} \right) \phi(t) = \Lambda^2\phi(t), \quad (12)$$

which is a Kummer equation that has exact solutions whose spectrum is given by

$$\Lambda_n^2 = 4n + 36, \quad n = 0, 1, 2, \dots$$

In Table 1 we see that the result from the exact and approximate calculation are quite different, thus the exponential in the potential is too strong to allow the simplified approximation.

n	0	1	2	3	...
Λ_n^2 (exact)	53.88	82.17	117.02	157.95	...
Λ_n^2 (approx)	36	40	44	48	...

Table 1: Exact versus approximate glueball modes

The numerical solution is very different from the approximate one as is clear from the potentials shown in the left panel of Fig. 1. One can see that for the approximate solution, the potential rises only for very large values of t and therefore the bound states are close to each other in energy, while the potential for exact solution rises for $t \sim 2$ thus the bound states are well separated in energy. Moreover, we see in the right panel of Fig. 1 that the behavior of the modes is also very different. In the exact solution, the dependence of the mass is linear with n in the low n region while in the approximation solution the mass squared is linear in n .

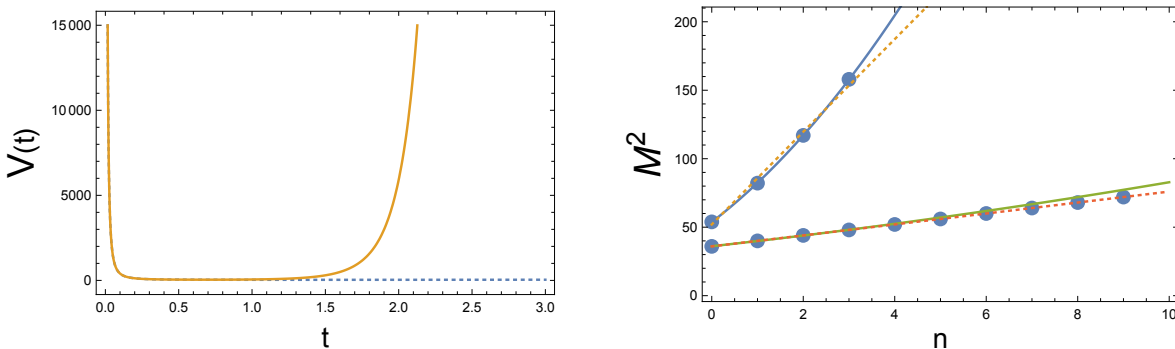


Figure 1: Left: We plot as a function of t the potentials of the equivalent exact (solid), Eq.(10), and approximate (dotted), Eq.(12), Schrödinger equations. Right: We plot the glueball modes of the exact solution and approximate solution noticing that the former is an almost linear relation with mass while the former is quadratic in mass in the region of our interest.

2.2 Mesons

In the case of the scalar mesons the variation of the action leads to

$$\partial_M(\sqrt{-g}e^{-\varphi(z)}g^{MN}\partial_N S(x, z)) = \sqrt{-g}e^{-\varphi(z)(1-\alpha)}M_{5m}^2 S(x, z). \quad (13)$$

Once we separate the x dependence by factorizing $S(x, z) = \Sigma(z)e^{-iq_\mu x^\mu}$ with $q^2 = -M^2$, where M is the mass of the meson modes, we get

$$-\frac{d^2\Sigma(z)}{dz^2} + \left(\frac{3}{z} + 2kz \right) \frac{d\Sigma(z)}{dz} + \frac{3}{z^2}e^{\alpha\varphi(z)}\Sigma(z) = M^2\Sigma(z) \quad (14)$$

where we have substituted the value of the scalar AdS_5 mass. By setting $\varphi(z) = kz^2$ and performing the change of function

$$\Sigma(z) = \left(\frac{z}{k}\right)^{\frac{3}{2}} e^{kz^2/2} \sigma(z), \quad (15)$$

we get a Schrödinger type equation

$$-\frac{d^2\sigma(z)}{dz^2} + \left(k^2 z^2 + 2k + \frac{15}{4z^2} - \frac{3}{z^2} e^{\alpha kz^2}\right) \sigma(z) = M^2 \sigma(z). \quad (16)$$

We now proceed to the change to the adimensional variable $u = \sqrt{k/2} z$,

$$-\frac{d^2\sigma(u)}{du^2} + \left(4u^2 + 4 + \frac{15}{4u^2} - \frac{3}{u^2} e^{2\alpha u^2}\right) \sigma(u) = \Lambda^2 \sigma(u). \quad (17)$$

Let us perform the same approximation as before, namely to expand the exponential and keep up to three terms to obtain

$$-\frac{d^2\sigma(u)}{du^2} + \left((4 - 6\alpha)u^2 + (4 - 6\alpha) + \frac{3}{4u^2}\right) \sigma(u) = \Lambda^2 \sigma(u). \quad (18)$$

This equation can be transformed into a Kummer type equation by the change of variables $v = (4 - 6\alpha)^{1/4} u$

$$-\frac{d^2\sigma(v)}{dv^2} + \left(v^2 + \frac{4 - 6\alpha}{\sqrt{4 - 6\alpha^2}} + \frac{3}{4v^2}\right) \sigma(v) = \frac{\Lambda^2}{\sqrt{4 - 6\alpha^2}}, \quad (19)$$

which has an exact spectrum given by

$$\Lambda_n^2 = 4(n + 1)\sqrt{4 - 6\alpha^2} + 4 - 6\alpha, \quad n = 0, 1, 2, \dots \quad (20)$$

and the mode functions are

$$\sigma(v) = \mathcal{N} e^{-v^2/2} v^{3/2} {}_1F_1(-n, 2, v^2) \quad (21)$$

where \mathcal{N} is a normalization factor and ${}_1F_1$ is a well known hypergeometric function and recall that $v = (4 - 6\alpha^2)^{1/4} u$ where $u = (\sqrt{k/2} z)$. Note that the approximate solution only has bound states for $|\alpha| < \sqrt{2/3}$.

The meson modes are a function of α . In the next section we will proceed to fix the parameters of the model by using phenomenological input. In Fig. 2 we show the exact lowest mode for $\alpha = 0.2$ (solid) together with the approximate solution obtained expanding the exponential to third order (dotted). For small values of α both solutions are very similar and their mode values almost equal. For larger values of $\alpha = 0.4$ closer to the no binding limit the mode values are very similar but the exact solution becomes unstable. We shall discuss these details further in the next section.

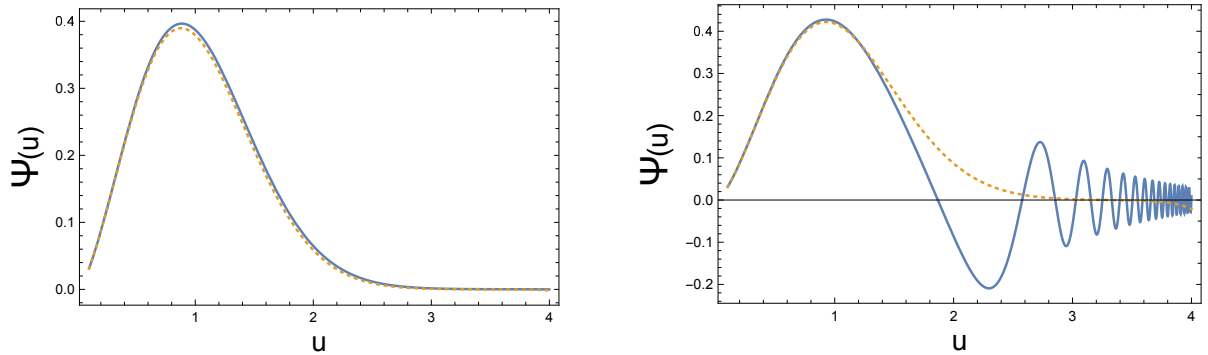


Figure 2: We plot as a function of u for $\alpha = 0.2$ (left) and $\alpha = 0.4$ (right) the exact solution for the lowest mode (solid), Eq.(17), and the approximate lowest mode solution (dotted) obtained by expanding in the exact mode equation the exponential to third order.

2.3 Phenomenological analysis

Our AdS/QCD model provides us with a succession of mass modes of differential equations which should be numerically solved. The equation for the glueballs Eq.(10) depends on a scale k which we will use to match the glueball spectrum obtained from lattice QCD in the quenched approximation which is Gluodynamics [20, 21, 22]. The equation for the mesons, Eq.(17), depends on k and α . We use the PDG spectrum to fit the mesons spectrum [23, 24], which is certainly QCD, if we assume that QCD is the theory of the strong interactions. In principle, the scale of the glueballs and the mesons should be the same if we could fit QCD data, but since we are using lattice QCD in the quenched approximation to fit the latter, one could expect some minor differences between the two. We will choose the same mass scale. The fitting procedure is different from that used before by many authors [6, 12, 18] where an overall scale was used since in this case the scale affects the mode functions, which correspond to the light cone wave functions[8], through the relation between the t and z variables.

We proceed to fit the glueball spectrum. The lattice data used are shown in Table 2 [20, 21, 22]¹. We also use for the fit the results for the tensor glueball states since the theory predicts degeneracy between the scalar and the tensor glueball for all soft-wall models. The value of the parameter, obtained in the fit shown in Fig. 3 with the GSW model, is $\alpha k = (370 \text{ MeV})^2$.

J^{PC}	0^{++}	2^{++}	0^{++}	2^{++}	0^{++}	0^{++}
MP	1730 ± 94	2400 ± 122	2670 ± 222			
YC	1719 ± 94	2390 ± 124				
LTW	1475 ± 72	2150 ± 104	2755 ± 124	2880 ± 164	3370 ± 180	3990 ± 277

Table 2: Glueball masses [MeV] from lattice calculations by MP [20], YC [21] and LTW [22].

Meson	$f_0(500)$	$f_0(980)$	$f_0(1370)$	$f_0(1500)$	$f_0(1710)$	$f_0(2020)$	$f_0(2100)$	$f_0(2200)$
PDG	475 ± 75	990 ± 20	1350 ± 150	1504 ± 6	1723 ± 6	1992 ± 16	2101 ± 7	2189 ± 13

Table 3: Scalar meson masses [MeV] from PDG [23, 24]

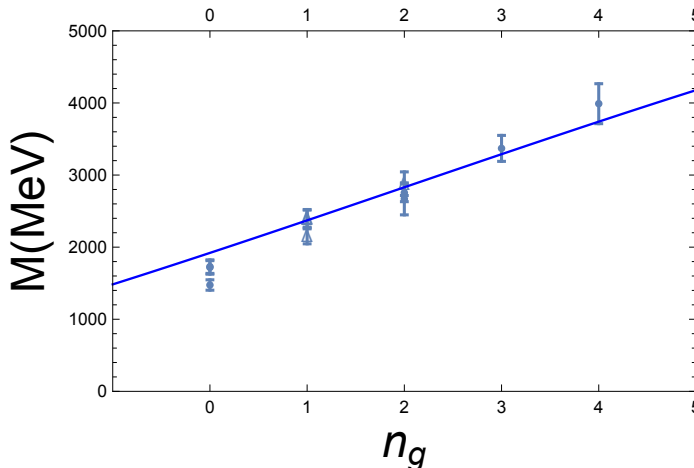


Figure 3: We plot the average lattice values for the scalar and tensor glueball masses of refs. [20, 21, 22] as a function of mode number. We show the fit to the spectrum from the modes of Eq. 10 by using just one parameter αk .

Now that αk has been fixed, we will use α to fit the meson spectrum. In order to estimate the value of α let us use the approximate equation Eq.(19) From the mode equation Eq.(20) we get the spectrum

$$M_n^2 = \Lambda_n^2 \frac{k}{2} = \Lambda_n^2 \frac{(370)^2}{2\alpha} . \quad (22)$$

¹We have not included the lattice results from the unquenched calculation [27] to be consistent, which however, in this range of masses and for these quantum numbers are in agreement with the shown results within errors.

Having this analytic equation the fitting procedure is quite straightforward. The first question is if we should include the $f_0(500)$ in the fit. As discussed in our work [19] many authors have argued it is not a conventional meson state but a tetraquark or a hybrid [28, 24]. In the present GSW model we have less freedom since the energy scale is fixed by the glueballs. In Fig. 4 we fit the PDG meson spectrum shown in Table 3 with our model. The left figure includes the $f_0(500)$ while the right figure does not.

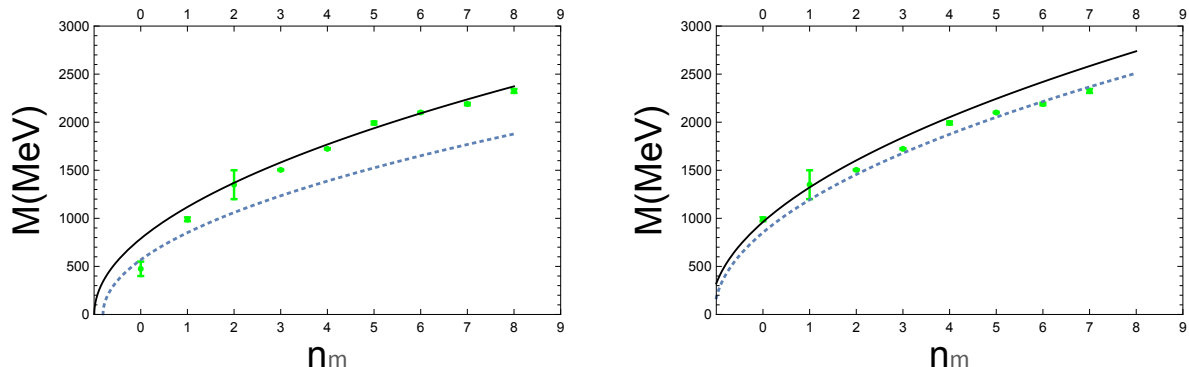


Figure 4: We plot the f_0 PDG meson spectrum [23, 24] as a function of mode number. Left: including the $f_0(500)$. The fits correspond to $\alpha = 0.67$ (solid) and $\alpha = 0.76$ (dotted). Right: without the $f_0(500)$. The fits correspond to $\alpha = 0.54$ (solid) and $\alpha = 0.63$ (dotted).

It is apparent again that the $f_0(500)$ is difficult to fit if the mass is so low as given in the PDG tables, and therefore probably the dynamical mechanism forming it is different from the rest of the mesons. From now on we will not consider the $f_0(500)$ in our fits to the meson spectrum.

The problem with the true solution, that corresponding to Eq.(17), is that it is very unstable as the binding potential becomes weaker, i.e. for values of $\alpha > 0.2$ and much more unstable for the higher modes as shown in Fig. 2. However, the spectrum does not differ much from the approximate spectrum and the mode functions have a similar structure before the large u oscillations appear. One should notice that the value for which the approximate solution starts to be different from the exact solution, $u > 1.5$, corresponds to $z > 10/\Lambda_{QCD}$. Thus for a strong confined system such region is of little relevance. In Fig. 5 we analyze the behavior of the mode values of the true solution. The dots represent the true solution. The upper points have been calculated for $\alpha = 0.1$ and the lower points for $\alpha = 0.2$. The lines represent the mode values of the approximate solution for $\alpha = 0.1$ (solid) and $\alpha = 0.3$ (dotted). Thus we see an almost perfect fit for $\alpha = 0.1$ but for $\alpha = 0.2$ the higher modes of the exact solution tend towards higher values of α of the approximate solution. If we look back to the right plot of Fig. 4 this is exactly what is happening, the lower values of the meson spectrum are fitted quite well by the approximate solution for $\alpha = 0.54$, while the upper modes are fitted by the solution for $\alpha = 0.63$. Having in mind these caveats from now on we will work with the approximate equation plotting not single curves but bands which take into account the difference between the true solution and the approximate solution.

One may conclude from the above analysis that the GSW model describes well both the scalar glueball and meson spectra with the same scale αk . It must be noted that the energy scale arises from the metric as does the α modification which builds up the mesons. Recall that this fit is $\mathcal{O}(N_C^0)$ and that corrections $\mathcal{O}(N_C^{-1})$ and higher should be added to obtain a precise value. However, the fact that the fit is quite good suggests that the contribution of the higher terms might be small.

In Fig. 6 we show the glueball lattice data (upper points) and the meson data (lower points). We plot also the fits with the GSW model discussed before and extend the fits to higher mode numbers to find that glueball masses with a certain mode number are equal to meson masses with a much larger mode number. For example, the glueball masses for $n_g = 0, 1, 2$ are similar to the scalar meson masses for $n_m = 4, 7, 10$ respectively. The difference in mode numbers grows as the masses of the glueballs increase due to the different slopes of the fitting curves. This observation has led us in a recent paper to discuss the meson glueball mixing scenario for high hadron masses [19]. We proceed to analyze the consequences of that observation in the GSW model

3 Glueball-Meson mixing

Scalar glueballs might mix with scalar mesons [28, 29]. Recently in view of the spectra of mesons and glueballs in AdS/QCD models we have discussed the possibility that at high energies mixing might not be favorable and states with mostly gluonic valence structure might exist [19]. This is an exciting possibility since the presence of almost pure glueball states and the study of their decays would help in understanding many properties of

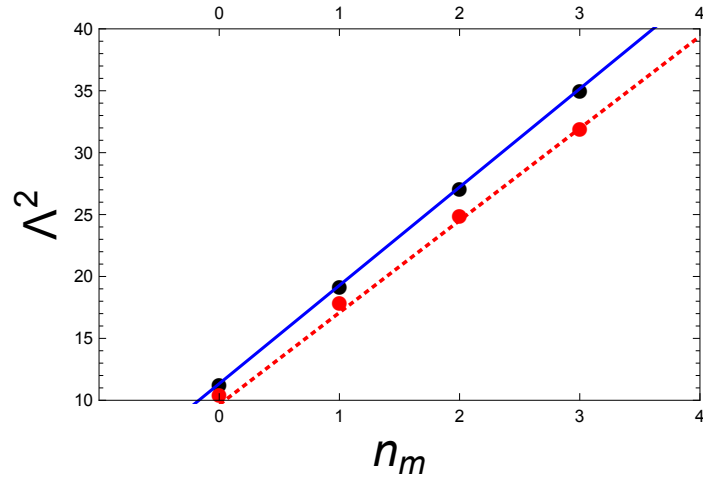


Figure 5: The dots represent the mode values of the true solution. The upper points correspond to $\alpha = 0.1$, the lower points to $\alpha = 0.2$. The lines represent the mode values of the approximate solution. The solid curve for $\alpha = 0.1$ the dotted curve for $\alpha = 0.3$.

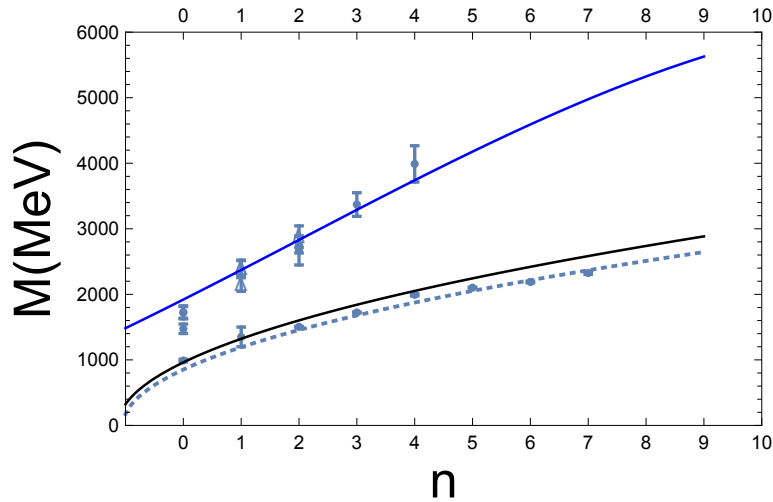


Figure 6: We show fits to the glueball spectrum (solid upper line) and scalar meson spectrum (lower band) obtained within the GSW model. The dark dots represent glueball spectrum obtained from lattice QCD [20, 21, 22]. The light dots represent the scalar meson spectrum obtained from experimental data [23, 24]. We have extended the fits to high mode numbers to motivate our analysis of mixing.

QCD related to the physics of gluons. In here we have described an AdS/QCD model in the scalar sector that describes both scalar mesons and scalar glueballs on an equal footing by means of a unique energy scale. This energy scale enters the description of the mode functions which can be interpreted, in the previously developed scheme, as a light cone wave functions. Let us recall the formalism.

The holographic light-front representation of the equation of motion, in *AdS* space can be recast in the form of a light-front Hamiltonian [8]

$$H_{LC}|\Psi_n\rangle = M^2|\Psi_n\rangle. \quad (23)$$

In the AdS/QCD light-front framework the above relation becomes a Schrödinger type equation

$$\left(-\frac{d^2}{dt^2} + V(t)\right)\Psi(t) = \Lambda^2\Psi(t) \quad (24)$$

where t and Λ^2 in this equation are adimensional. The holographic light-front wave functions are defined by $\Psi_n(t) = \langle t|\Psi_n\rangle$ and are normalized as

$$\langle \Psi_n|\Psi_n\rangle = \int dt |\Psi_n(t)|^2 = 1 \quad (25)$$

The described mode functions introduce, in this way, probability distributions.

The eigenmodes of Eq.(24) determine the mass spectrum. In this framework, we get functions of t for which we can define a probability distributions as in Eq.(25). In ref. [19] we discussed the mixing in a two dimensional Hilbert space generated by a meson and a glueball states, $\{|\Psi_m\rangle, |\Phi_g\rangle\}$. We found out that the mixing probability is proportional to the overlap probability of these two wave functions, i.e $|\langle\Psi_m|\Phi_g\rangle|^2$. Thus in order to discuss mixing we need the mode functions. In the case of the glueballs we find the mode functions numerically since we have shown that the approximate solution is very different from the exact one, while in the meson case we use the approximate solution, which behaves similarly, with some caveats, to the exact mode function. The meson equation can be brought into Kummer's form Eq.(19) by a convenient change of variables in terms of which the the mode functions are given by Eq.(21).

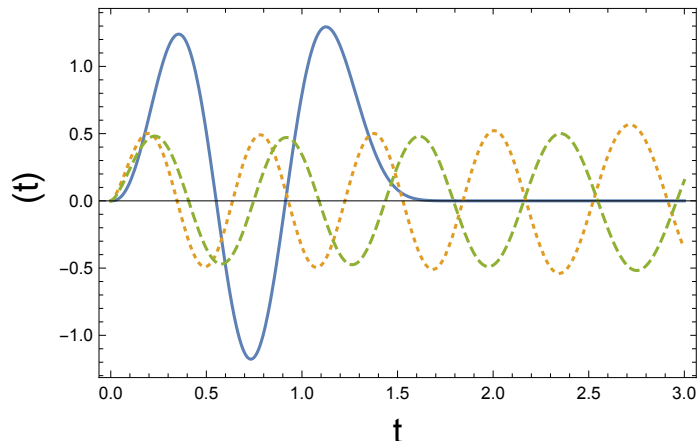


Figure 7: We plot the glueball mode function for $n_g = 2$ and the meson mode functions for $n_m = 10$ and $\alpha = 0.54$ (dashed) and $\alpha = 0.63$ (dotted).

In Fig. 8 we plot the probability of no mixing for low lying glueball modes ($n_g = 1, 2, 3$) overlapping with mesons of modes up to mode number $n_m = 10$. We observe that the overlap probability is small for the larger meson mode numbers and that it is only sizeable when the mode numbers of the two states are not very different. Let us make the discussion more detailed with an example. We choose a glueball of mode number $n_g = 2$ and a meson of mode number $n = 10$. They can be considered as candidates for mixing because the glueball mass in the model is $m(n_g = 2) \sim 2800$ MeV and the meson mass is also $m(n_m = 10) \sim 2800$ MeV. Thus this example is a prototype for a mixing scenario for heavy particles. In Fig.7 we show the mode functions for the $n_g = 2$ glueball mode and that for the $n_m = 10$ meson mode for the GSW model as a function of t . We note that the meson function oscillates rapidly due to its larger mode number and therefore the overlap integral becomes very small. Note that the true mode function will be in between those two drawn, closer to the one of shorter wavelength for low modes and to the one of longer wavelength for the higher modes.

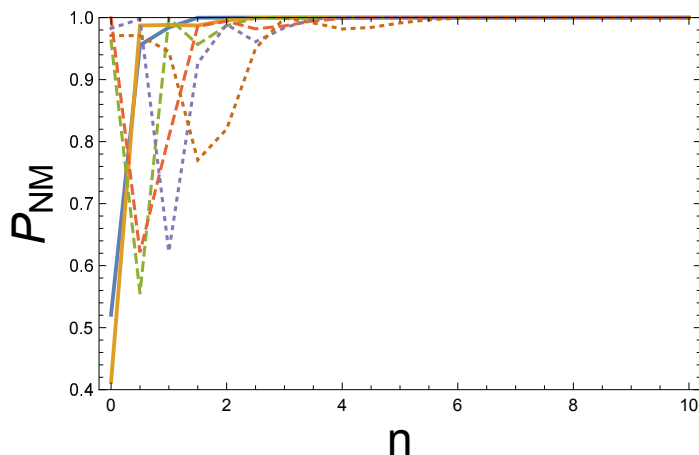


Figure 8: We plot the probability of no mixing for the glueball with mode numbers $n_g = 0$ (solid), 1 (dotted), 3 (dot-dashed), as a function of meson mode number n_m

Looking at Figs. 6 and 8, we see that a favorable mixing scenario is mostly excluded in the case of heavy glueballs and mesons, since the mass condition is satisfied for very different mode numbers. For example it can be seen that for $n_g = 2, 3, 4$ the favorable meson modes of almost equal masses occur for $n \sim 10, 13, 17$. The outcome of our analysis is that the AdS/QCD approach predicts the existence of almost pure glueball states in the scalar sector in the mass range above 2 GeV.

4 Conclusion

In this work we have discussed the application of Graviton Soft Wall Model for both scalar glueballs and mesons. To this aim, we have compared the theoretical spectrum with lattice QCD data in the case of the glueballs and the experimental f_0 spectrum of the PDG tables in the case of the mesons. The model introduces a unique energy scale for both glueballs and mesons. We have shown that the model respects the Regge behavior and nicely reproduces both these spectra at leading order in $1/N_c$.

We have noted that in this model the slope of the glueball spectrum, as a function of mode number, is also bigger than that of the meson spectrum and therefore for heavy almost degenerate glueballs and mesons states, their mode numbers differ considerably. Assuming a light-front quantum mechanical description of AdS/QCD correspondence, we have shown that the overlap probability of heavy glueballs to heavy mesons is small and thus one expects little mixing in the high mass sector. Therefore, this is the kinematical region to look for almost pure glueball states. At present stage, large statistics of Central Exclusive Process (CEP) data is being collected by the LHC experiments, and we expect exciting new results to appear concerning the higher mass gluon enriched process.

Acknowledgments

We acknowledge Sergio Scopetta and Marco Traini for discussions. VV thanks the hospitality extended to him by the University of Perugia and the INFN group in Perugia. This work was supported in part by MICINN and UE Feder under contract FPA2016-77177-C2-1-P, and by the STRONG-2020 project of the European Unions Horizon 2020 research and innovation programme under grant agreement No 824093.

References

- [1] J. M. Maldacena, *Int. J. Theor. Phys.* **38**, 1113 (1999)
- [2] E. Witten, *Adv. Theor. Math. Phys.* **2**, 505 (1998)
- [3] H. Fritzsche, M. Gell-Mann and H. Leutwyler, *Phys. Lett.* **47B** (1973) 365.
- [4] H. Fritzsche and P. Minkowski, *Phys. Lett.* **56B** (1975) 69.
- [5] V. Vento, *Eur. Phys. J. A* **53** (2017) no.9, 185
- [6] M. Rinaldi and V. Vento, *Eur. Phys. J. A* **54**, 151 (2018)
- [7] J. Polchinski and M. J. Strassler, hep-th/0003136.
- [8] S. J. Brodsky and G. F. de Teramond, *Phys. Lett. B* **582** (2004) 211
- [9] L. Da Rold and A. Pomarol, *Nucl. Phys. B* **721** (2005) 79
- [10] A. Karch, E. Katz, D. T. Son and M. A. Stephanov, *Phys. Rev. D* **74** (2006) 015005
- [11] J. Erlich, E. Katz, D. T. Son and M. A. Stephanov, *Phys. Rev. Lett.* **95** (2005) 261602
- [12] P. Colangelo, F. De Fazio, F. Giannuzzi, F. Jugeau and S. Nicotri, *Phys. Rev. D* **78** (2008) 055009
- [13] G. F. de Teramond and S. J. Brodsky, *Phys. Rev. Lett.* **94**, 201601 (2005).
- [14] M. Rinaldi, *Phys. Lett. B* **771**, 563 (2017)
- [15] A. Bacchetta, S. Cotogno and B. Pasquini, *Phys. Lett. B* **771**, 546 (2017)
- [16] G. F. de Teramond *et al.* [HLFHS Collaboration], *Phys. Rev. Lett.* **120**, no. 18, 182001 (2018)
- [17] P. Colangelo, F. De Fazio, F. Jugeau and S. Nicotri, *Phys. Lett. B* **652** (2007) 73

- [18] E. Folco Capossoli and H. Boschi-Filho, Phys. Lett. B **753**, 419 (2016)
- [19] M. Rinaldi and V. Vento, arXiv:1803.05738 [hep-ph].
- [20] C. J. Morningstar and M. J. Peardon, Phys. Rev. D **60** (1999) 034509
- [21] Y. Chen, A. Alexandru, S. J. Dong, T. Draper, I. Horvath, F. X. Lee, K. F. Liu and N. Mathur *et al.*, Phys. Rev. D **73** (2006) 014516
- [22] B. Lucini, M. Teper and U. Wenger, JHEP **0406** (2004) 012
- [23] C. Patrignani *et al.* [Particle Data Group], Chin. Phys. C **40** (2016) no.10, 100001.
- [24] M. Tanabashi *et al.* [Particle Data Group], Phys. Rev. D **98** (2018) no.3, 030001.
- [25] T. Gutsche, V. E. Lyubovitskij, I. Schmidt and A. Y. Trifonov, Phys. Rev. D **99**, no. 5, 054030 (2019)
- [26] A. Vega and P. Cabrera, Phys. Rev. D **93**, no. 11, 114026 (2016)
- [27] E. Gregory, A. Irving, B. Lucini, C. McNeile, A. Rago, C. Richards and E. Rinaldi, JHEP **1210** (2012) 170
- [28] V. Mathieu, N. Kochelev and V. Vento, Int. J. Mod. Phys. E **18** (2009) 1
- [29] V. Vento, Eur. Phys. J. A **52** (2016) no.1, 1